Proceedings of the 33rd European Safety and Reliability Conference (ESREL 2023)
Edited by Mário P. Brito, Terje Aven, Piero Baraldi, Marko Čepin and Enrico Zio

doi: 10.3850/978-981-18-8071-1_P251-cd

Transient thermal analysis, test verification and structural optimization on the integrated flywheel

Ning Zhang

Development Center of On-Board Computer and Electronics, Beijing Institute of Control Engineering, China. E-mail: married090625@163.com

Haibin Li

Development Center of On-Board Computer and Electronics, Beijing Institute of Control Engineering, China. E-mail: lhbboy0@126.com

Yiyun Xi

Development Center of On-Board Computer and Electronics, Beijing Institute of Control Engineering, China. E-mail: ayun0604@foxmail.com

Pengbo Zhang

Development Center of Mechatronics, Beijing Institute of Control Engineering, China. E-mail: billow1230@163.com

Jun Li

Development Center of On-Board Computer and Electronics, Beijing Institute of Control Engineering, China. E-mail: 13466396169@163.com

Yaqi Song

Development Center of On-Board Computer and Electronics, Beijing Institute of Control Engineering, China. E-mail: 7032426@qq.com

Jian Yang

Development Center of On-Board Computer and Electronics, Beijing Institute of Control Engineering, China. E-mail: yanzi1227@163.com

Lan Zhao

Development Center of On-Board Computer and Electronics, Beijing Institute of Control Engineering, China. E-mail: zhlanlandjh@126.com

Fang Yu

Development Center of On-Board Computer and Electronics, Beijing Institute of Control Engineering, China. E-mail: 17396799@qq.com

With the requirement of agility and miniaturization to the aerospace industry, the high-integration concept has been widely applied to design the mechanic-electric products. Taking the flywheel as an example, the mechanism and the control parts are achieved to merge together in recent years. Meanwhile, the maneuvering condition of the flywheel usually induces to higher heat consumption and more rigid thermal reliability on the components. In order to protect the product and reduce the failure risk, it is necessary to analyze the transient thermal distribution of the flywheel and the dissipating paths of the PCB layout by simulation. Additionally, it is feasible to improve the thermal reliability by using structural optimization methods. Based on the statement above, the transient thermal analysis of the integrated flywheel is conducted and the simulation model is established by FEA software.

Under the maneuvering conditions, the influence of heat consumption variation on the flywheel's circuit is paid more attention. Temperature-time curves of concerned components are plotted and the location of highest temperature value is pointed out. Then, thermal balancing test is operated to verify the simulation accuracy. It is summarized that the simulation results have a good consistence with the test data, and the computational errors are mainly less than 3°C. Finally, the structural optimization on the component placement is carried out to improve the thermal reliability of the integrated flywheel.

Keywords: aerospace industry, integrated flywheel, maneuvering condition, transient thermal analysis, test verification, structural optimization.

1. Introduction

With trends of miniaturization and agility on the aerospace industry, the high-integration concept has been widely applied to design the conventional mechanic-electric products. Taking the flywheel as an example, the brand-new ones have been achieved a combination of the mechanism and the circuit. Meanwhile, the control and the power supply parts have been amounted on one board by the high-integration design.

In addition, acting as an actuator, the requirements of the agility and the high frequent maneuvering are significant during the on-orbit service of the flywheel, which requires a higher reliability consideration on the circuit thermal design. Due to the limitation of heat flux, the heat concentration on the PCB board is totally increased and the influence of transient heat on the components should be paid more attention. Thus, the feasible design of the dissipating path is very important. As known that, it is hard to dissipate heat in the space due to the lack of convection. Generally speaking, the high heat flux components are usually fixed nearby the cold plate on the satellite in order to reduce the dissipating paths and improve the dissipating effect. Based on mentioned above, the transient thermal simulation of the integrated flywheel is carried out at the preliminary design phase. Usually, the simulation results are used to conduct the structural design and dissipating path improvement. Moreover, the accurate simulation model is utilized to compare and estimate the heat distributions of components under different conditions and finally applied to replace some of the real experiments.

In this paper, the transient thermal analysis on the integrated flywheel is performed under two consecutive conditions. The temperature contours of concerned components are obtained and the temperature-time curves are plotted. Location and value of the highest temperature in the flywheel are found. In order to verify the accuracy of simulation model, the heat balancing test is conducted and the actual temperatures of the concerned components are measured by employing the thermocouples. With the help of simulation, the heat dissipation optimization is iterated to improve the thermal reliability of the integrated flywheel.

2. Methodologies

Bases on the theory of heat transfer, the conventional vector differential equation in the non-steady state and inner heat power condition was shown as follows:

$$\rho c_P \frac{\partial t}{\partial \tau} = \lambda\left(\frac{\partial^2 t}{\partial x^2} + \frac{\partial^2 t}{\partial y^2} + \frac{\partial^2 t}{\partial z^2}\right) = \lambda \mathrm{div}(\mathrm{grad}\ t) + \dot{\Phi} \qquad (1)$$

Where $\mathrm{div}(\mathrm{grad\ t})$ or $\nabla^2 \mathrm{t}$ was the Laplace factor of temperature. When the ρc_P value was constant, the heat diffusivity was inserted as $a = \frac{\lambda}{\rho c_P}$ and the equation 1 could be rewritten below:

$$\frac{\partial t}{\partial \tau} = a\nabla^2 t + \frac{\dot{\Phi}}{\rho c_P} \qquad (2)$$

From the equation 2, it was easy to find that the parameters of heat conductivity, density and specific heat need to assign when conducted the transient thermal analysis. The energy equilibrium equation was described by matrix as follows:

$$[C]\{\dot{T}\} + [K]\{T\} = \{Q\} \qquad (3)$$

Where $[C]$ was the specific heat matrix, $\{\dot{T}\}$ was the derivative of temperature to time, $[K]$ was the heat conductivity matrix, in which included conductivity factor, convection factor, radiation and geometry factor, $\{T\}$ was the temperature vector, $\{Q\}$ was the heat flux vector.

During the transient thermal analysis, the temperature, the boundary condition, the heat flux and the inner energy of system were remarkably changed with time. Considering that the space was a vacuum atmosphere, the influence of convection was ignored when defined the boundary condition.

In addition, there were many micro-gaps on the surfaces of contacting objects in the actual heat conduction process, which caused a certain thermal resistance. Usually, the contacting conductivity coefficient T_{CC} was defined to evaluate the contacting thermal resistance value. When the heat transferred on surfaces of different mediums, the relationship between the heat energy and temperature was described as follows:

$$q = \frac{Q}{A} = T_{CC}\,(T_{target} - T_{contact}) \qquad (4)$$

Where $T_{contact}$ was the temperature of a contacting node, T_{target} was the temperature of corresponding node, the typical unit of T_{CC} was W/m^2·K.

3. Analysis and results

Main structure of integrated flywheel was made of 2A12 aluminum alloy, which included the circuit control and the wheel mechanism, as shown in Fig 1.

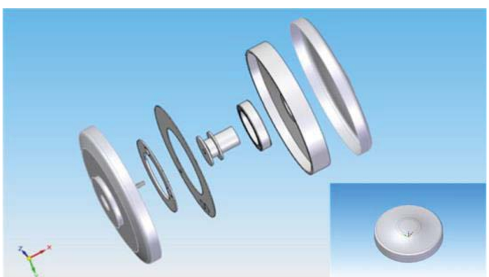

Fig 1 Main structure of integrated flywheel

In the view of the high frequency maneuvering requirement, two typical thermal load conditions were selected to conduct the transient heat transfer analysis as shown in Fig 2. Commonly, peak heat dissipation of the flywheel was mainly occurred on the transient maneuvering process. Considering the existence of heat capacity, four periodical transient thermal cycles were determined to simulate by using FEA software, in order to reach the dynamic stability on temperatures of the whole product and the components. Material properties of the flywheel were listed in table 1. Ambient temperature of the flywheel was in a range of -5°C+45°C. Therefore, the worst case in the simulation work was defined to 45°C on the heat sink as a boundary condition.

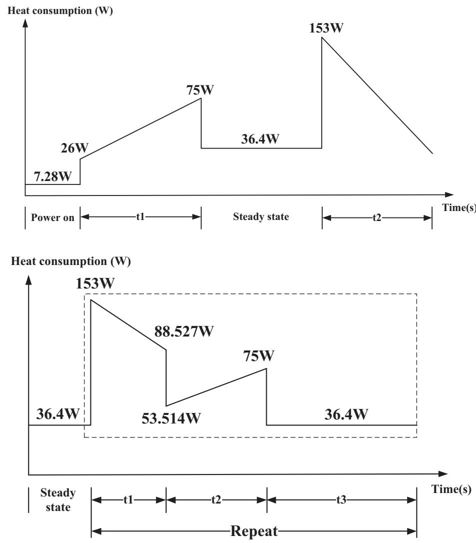

Fig 2 Two typical thermal loading conditions of the flywheel

Table 1 Material properties of the flywheel

No	Material	Heat conduction coefficient [W/(m·K)]	Emissivity ε_h	Density (kg/m^3)	Specific heat [J/(kg·K)]	Remarks
1	Al alloy (2A12)	114	0.04	2770	875	Emissivity of the outer housing is 0.85
2	Copper	398	0.06	8300	385	/
3	FR4	0.4	0.9	2520	880	/
4	Component	16	0.04	3970	765	/

5	Stainless steel	15.1	0.20	7750	480	/

The components concerned in this simulation were listed in table 2, the power components were directly amounted on the structure and the heat sources of others were evenly distributed on the PCB boards. Besides, heat sources of the electric motor and the bearings were equilibrated to assign by the body heat source in transient thermal analysis.

Table 2 Concerned components on the PCB boards

No	Reference designator	Category	Packaging pattern	Thermal resistance R_{J-C} (°C/W)	Derating temperature (°C)
1.	V101	Power tube	TO-254	0.5	90
2.	V103	Power tube	TO-254	0.5	90
3.	D108\D109	Power diode	TO-254	0.5	90
4.	D103	Power diode	SMD-0.5	3.5	90
5.	IC101	PWM	DIP-16	20.7	85
6.	D4	Diode	TO-254	0.5	90
7.	Q14	Power tube	TO-254	0.5	90
8.	Q12\Q12A	Transistor	TO-39	35	115
9.	L1	Inductor	/	/	130

Transient heat transfer algorithm in the FEA software was applied. Due to the difference of the packaging pattern, the contacting conductance coefficients of components and materials should be highly focused during the model definition process. Total number of node was 92510 and total number of element was 56184. The entire structure was partitioned by using hexahedral elements, as shown in Fig 3.

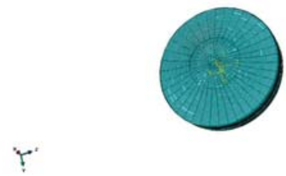

Fig 3 Integrated flywheel structure after meshing

The heat consumptions of components were defined by the body flux, and the radiation heat exchange was considered on the surfaces of materials. The transient thermal conditions were assigned in Fig 2. After calculation convergence, the final temperature distributions of the entire structure in two cases were illustrated, as shown in Fig 4. From the contour results, it was obvious that the high temperature zones were mainly located at the bearings and the stators. It was summarized that the peak temperatures on the PCB board in two cases were located at Q12 and Q12A, respectively. The highest values were 61.4°C and 64.6°C.

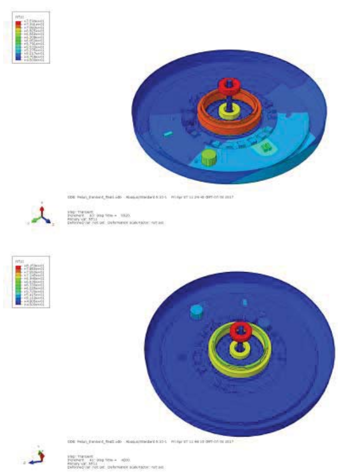

Fig 4 Thermal distribution contours of flywheel in two cases

Meanwhile, the temperature-to-time curves of components concerned in two cases were plotted in Fig 5. From trend of the curves, it was seen that the temperatures of components were gradually stabilized after several loading cycle iterations.

From the analysis of simulation curves, the temperature changes of components were relatively minor after several cycles. It was indicated that the temperatures have been stabilized and the simulation results could be summarized to compare with the experimental ones. Therefore, the simulation results were summarized and compared to the ones of heat balancing tests.

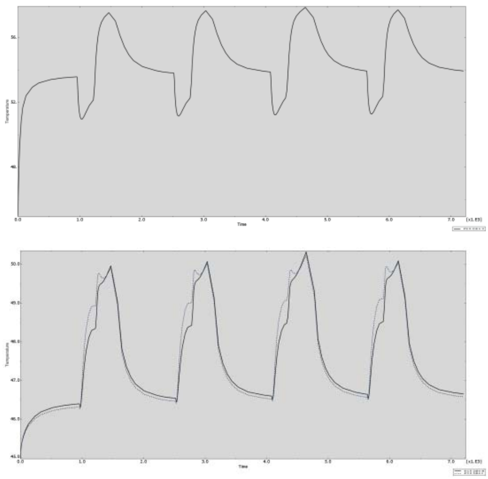

Fig 5 Typical transient temperature curves of concerned components in two cases

4. Verification and optimization

In order to verify the simulation results, the thermal balancing test was conducted at 45±0.5°C and the temperature of the outer housing was controlled at 40±0.5°C. Transient thermal balancing test was begun after keeping conditions when the temperature change rate is less than 0.1°C/h or the temperature absolute value is less than 0.5°C. In this research, two kinds of data were summarized to verify the accuracy of simulation analysis. One was the highest temperature values of selected components in the stable thermal condition. The other one was the temperature to time curves of selected components in the transient maneuvering condition. It was found that the simulation and the test data had a good correspondence, and the computational error was approximately less than 3°C, as listed in table 3.

Table 3 Computational error of simulation and experimental

No	Reference designator	Simulation (°C)		Experimental (°C)		Error (°C)	
		Case1	Case2	Case1	Case2	Case1	Case2
1.	V101	48.4	49	47.3	50.5	1.1	1.5
2.	V103	49.7	50.4	48.8	53.2	0.9	2.8
3.	D108	48.7	49.4	48.9	52.3	0.2	2.9
4.	D109	49.5	49.8	48.9	52.7	0.6	2.9
5.	D103	51.0	51.7	48.5	52.7	2.5	1
6.	IC101	56.6	57.5	55.9	58.5	0.7	1
7.	D4	56.3	55.6	55.6	55.4	0.7	0.2
8.	Q14	53.1	52.7	55.2	54.5	2.1	1.8
9.	Q12	61.4	64.2	58.5	61.7	2.9	2.9
10.	Q12A	61.1	64.6	57.8	60.8	3.3	3.4
11.	L1	65.7	70.7	63.1	70.5	2.6	0.2

After the accuracy confirmation, the genetic algorithm theory was applied to optimize the component layout and thermal distribution. It is well-known that, Genetic Algorithms (GAs) are a type of trial-and-error search technique that are guided by principles of Darwinian evolution. Just as the genetic material of two living organisms can intermix to produce offspring that are better adapted to their environment, GAs expose genetic material, frequently strings of 1s and 0s, to the forces of artificial evolution: selection, mutation, recombination, etc. Firstly, GAs start with a pool of randomly-generated candidate solutions, which are then tested and scored with respect to their utility. Then, solutions are bred by probabilistically selecting high quality parents and recombining their genetic representations to produce offspring solutions. Offspring are typically subjected to a small amount of random mutation. Lastly, after a pool of offspring is produced, this process iterates until a satisfactory solution is found or an iteration limit is reached. Genetic algorithms have been applied to a wide variety of problems in many engineering fields.

In this research, the Archive-based Micro Genetic Algorithm (AMGA) is used to optimize the PCB layout, which is an evolutionary optimization algorithm that relies on genetic variation operators for creating new solutions. The algorithm uses the concept of Pareto ranking borrowed from Non-dominated Sorting Genetic Algorithm (NSGA-II) and is based on a two-tier fitness mechanism, which mainly solves the Multiple-objective Optimization Problem (MOP). The generation scheme deployed in AMGA can be classified as generational since, during a particular iteration (generation), only solutions created before that iteration take part in the selection process. However, the algorithm generates a very small number of new solutions (it can work with just two solutions per iteration) at every iteration. Therefore, it can also be classified as an almost steady-state genetic algorithm. This attribute helps the algorithm achieve faster convergence than most generational genetic algorithms. The basic flowchart of the algorithm is as follows:

1) Begin operations.
2) Generate the initial population.
3) Evaluate the initial population.
4) Update the archive (using the initial population).
5) Repeat the following steps...
    a) Create the parent population from the archive.
    b) Create the mating pool from the parent population.
    c) Create the offspring population from the mating pool.
    d) Evaluate the offspring population.
    e) Update the archive (using the offspring population).
6) ...until termination is reached.
7) Report the desired number of solutions from the archive.
8) End operations.

Following the method above, the engineering practice was conducted in optimization software, as shown in Fig 6. The flow was established and the simulation model was linked to iterate as the definition of AMGA.

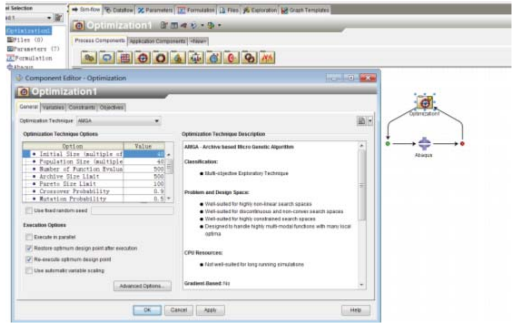

Fig 6 Simple establishment of optimization model calculated by AMGA

Finally, the optimization result of the PCB layout is displayed in Fig 7. Some of the components have been changed the location to improve the heat distribution during the transient maneuvering condition, as shown in the figure by the dotted line.

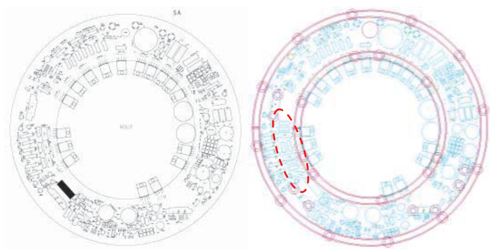

Fig 7 Comparison of flywheel's PCB layout using the optimization theory

5. Conclusions

According to the transient thermal analysis of the integrated flywheel, the temperature variation ranges of the concerned components were determined and the temperature-time curves were plotted. Based on the experimental data of the thermal balancing tests, the simulation modeling and results were compared and verified. It was shown that the computational errors were almost less than 3°C, which achieved the effective prediction of heat performance on the integrated flywheel. The heat reliability designs of all components were reached to the derating requirements, which supported an efficient method to improve the design capability of the integrated flywheel.

References

J. P. Holman (2011). *Heat transfer* (10th ed.). McGraw-Hill Publication.

Kyle Glenn Strohmaier (2014, July). Modeling, Optimization, and Detailed Design of a Hydraulic Flywheel-Accumulator. Master dissertation, University of Minnesota.

Shijie Xu, Naigang Cui (2018). Active Vibration Suppression of Flexible Spacecraft During Attitude Maneuver With Actuator Dynamics. *IEEE Access*, 35327-35337.

AntonioDella Gatta, LuigiIannelli (2018). A survey on modeling and engagement control for automotive dry clutch, *Mechatronics*, 63-75.

Hiroyuki Yoshihara and Masaki Takahashi (2019). Satellite Attitude Control and Power Tracking with VSCMGs During Large-angle and Agile Attitude Maneuvers, *12th Asian Control Conference*, 1613-1618.

Karpenko Mark, Lippman Travis (2019). Fast Attitude Maneuvers for the Lunar Reconnaissance Orbiter, AAS 19-053.

Abaqus Analysis User's Guide, *ABAQUS 6.17*.

Giuseppe Cataldo, Malcolm B. Niedner, Dale J. Fixsen, Samuel H. Moseley (2017). Model-based thermal system design optimization for the James Webb Space Telescope.

S. Kirkpatrick, C. D. Gelatt, and M. P. Vecchi (1983), Optimization by Simulated Annealing, *Science 220(4598)*, 671–680.

J. Holland (1975), Adaptation in Natural and Artificial Systems, University of Michigan Press.

F. Jouffroy and N. Durand (2007), Thermal model correlation using genetic algorithms, 21st European Workshop on Thermal and ECLS Software, 125–138.